Poznań University of Technology

Doctoral Thesis

Method for direct noise analysis of transonic axial compressor blade

Author:
MSc. Eng. Jędrzej Mosiężny

Supervisor:
Prof. DSc. Eng. Michał Ciałkowski

A thesis submitted in fulfilment of the requirements for the degree of Doctor of Philosophy. Engineer.

in the

Faculty of Work Machines and Transportation
Chair of Thermal Engineering

August 6, 2018

Declaration of Authorship

I, MSc. Eng. Jędrzej Mosiężny, declare that this thesis titled, 'Method for direct noise analysis of transonic axial compressor blade' and the work presented in it are my own. I confirm that:

- This work was done wholly or mainly while in candidature for a research degree at this University.
- Where any part of this thesis has previously been submitted for a degree or any other qualification at this University or any other institution, this has been clearly stated.
- Where I have consulted the published work of others, this is always clearly attributed.
- Where I have quoted from the work of others, the source is always given. With the exception of such quotations, this thesis is entirely my own work.
- I have acknowledged all main sources of help.
- Where the thesis is based on work done by myself jointly with others, I have made clear exactly what was done by others and what I have contributed myself.

Signed:

Date:

Abstract

This thesis proposes a method of assessing flow generated noise in transonic flows by direct formulation.

First a steady state Reynolds Averaged Navier-Stokes analysis of NASA R67 transonic axial compressor is performed as a validation study of the mesh and numerical setup. The result of the steady state analysis is then used as an initialization for transient DDES analysis performed on high quality, 11 million cells hexagonal mesh. The transient analysis covers 0.05s of physical flow time, which corresponds to about 800 revolutions of the rotor. Both steady state and transient simulations are performed on PL-Grid HPC infrastructure.

Transient results are analyzed with an in-house build program. The program uses information about static pressure, transient particle velocity and vorticity from each timestep. This data is then postprocessed into sound pressure levels, sound frequency and effective sound power level.

Information on generation of sound phenomena occurring in the blade passage are gathered from direct formulation and may be used as a validation case for FW-H or other computational aeroacoustic analogies dealing with flows in transonic regimes in rotating machinery.

Acknowledgements

In this place I would like to thank the Chair of Thermal Engineering of Poznań University of Technology, with special recognition to MSc. Eng. Bartosz Ziegler and PhD Eng. Przemysław Grzymisławski for thorough scientific and personal support during this project.

A big recognition goes to the owners and maintainers of the PLGRID - Polish HPC infrastructure, especially team in HPC Cyfronet center in AGH University of Science and Technology in Kraków. Being able to use the state of the art HPC clusters for analyses made this project possible.

Contents

List of Figures

List of Tables

Abbreviations

CAA	**C**omputional **A**ero **A**coustics
CFD	**C**omputional **F**luid **D**ynamics
DDES	**D**elayed **D**etached **E**ddy **S**imulation
DES	**D**etached **E**ddy **S**imulation
HPC	**H**ight **P**ower **C**omputing
LES	**L**arge **E**ddy **S**imulation
N-S	**N**avier **S**tokes
SRS	**S**cale **R**resolving **S**imulation

Physical Constants

Speed of Light $c = 2.997\ 924\ 58 \times 10^8\ \mathrm{ms}^{-\mathrm{S}}$ (exact)

Symbols

a	distance	m
P	power	W (Js^{-1})
ω	angular frequency	$rads^{-1}$

To my wife. For limitless patience...

Chapter 1

Introduction

1.1 Main Section 1

Lorem ipsum dolor sit amet, consectetur adipiscing elit. Aliquam ultricies lacinia euismod. Nam tempus risus in dolor rhoncus in interdum enim tincidunt. Donec vel nunc neque. In condimentum ullamcorper quam non consequat. Fusce sagittis tempor feugiat. Fusce magna erat, molestie eu convallis ut, tempus sed arcu. Quisque molestie, ante a tincidunt ullamcorper, sapien enim dignissim lacus, in semper nibh erat lobortis purus. Integer dapibus ligula ac risus convallis pellentesque.

Lorem ipsum dolor sit amet, consectetur adipiscing elit. Aliquam ultricies lacinia euismod. Nam tempus risus in dolor rhoncus in interdum enim tincidunt. Donec vel nunc neque. In condimentum ullamcorper quam non consequat. Fusce sagittis tempor feugiat. Fusce magna erat, molestie eu convallis ut, tempus sed arcu. Quisque molestie, ante a tincidunt ullamcorper, sapien enim dignissim lacus, in semper nibh erat lobortis purus. Integer dapibus ligula ac risus convallis pellentesque.

1.1.1 Subsection 1

Nunc posuere quam at lectus tristique eu ultrices augue venenatis. Vestibulum ante ipsum primis in faucibus orci luctus et ultrices posuere cubilia Curae; Aliquam erat volutpat. Vivamus sodales tortor eget quam adipiscing in vulputate ante ullamcorper. Sed eros ante, lacinia et sollicitudin et, aliquam sit amet augue. In hac habitasse platea dictumst.

1.1.2 Subsection 2

Morbi rutrum odio eget arcu adipiscing sodales. Aenean et purus a est pulvinar pellentesque. Cras in elit neque, quis varius elit. Phasellus fringilla, nibh eu tempus

venenatis, dolor elit posuere quam, quis adipiscing urna leo nec orci. Sed nec nulla auctor odio aliquet consequat. Ut nec nulla in ante ullamcorper aliquam at sed dolor. Phasellus fermentum magna in augue gravida cursus. Cras sed pretium lorem. Pellentesque eget ornare odio. Proin accumsan, massa viverra cursus pharetra, ipsum nisi lobortis velit, a malesuada dolor lorem eu neque.

1.2 Main Section 2

Sed ullamcorper quam eu nisl interdum at interdum enim egestas. Aliquam placerat justo sed lectus lobortis ut porta nisl porttitor. Vestibulum mi dolor, lacinia molestie gravida at, tempus vitae ligula. Donec eget quam sapien, in viverra eros. Donec pellentesque justo a massa fringilla non vestibulum metus vestibulum. Vestibulum in orci quis felis tempor lacinia. Vivamus ornare ultrices facilisis. Ut hendrerit volutpat vulputate. Morbi condimentum venenatis augue, id porta ipsum vulputate in. Curabitur luctus tempus justo. Vestibulum risus lectus, adipiscing nec condimentum quis, condimentum nec nisl. Aliquam dictum sagittis velit sed iaculis. Morbi tristique augue sit amet nulla pulvinar id facilisis ligula mollis. Nam elit libero, tincidunt ut aliquam at, molestie in quam. Aenean rhoncus vehicula hendrerit.

Chapter 2

Current research on Computational Aeroacoustics

2.1 Main Section 1

Lorem [1] ipsum dolor sit amet, consectetur adipiscing elit. Aliquam ultricies lacinia euismod. Nam tempus risus in dolor rhoncus in interdum enim tincidunt. Donec vel nunc neque. In condimentum ullamcorper quam non consequat. Fusce sagittis tempor feugiat. Fusce magna erat, molestie eu convallis ut, tempus sed arcu. Quisque molestie, ante a tincidunt ullamcorper, sapien enim dignissim lacus, in semper nibh erat lobortis purus. Integer dapibus ligula ac risus convallis pellentesque.

2.1.1 Subsection 1

Nunc posuere quam at lectus tristique eu ultrices augue venenatis. Vestibulum ante ipsum primis in faucibus orci luctus et ultrices posuere cubilia Curae; Aliquam erat volutpat. Vivamus sodales tortor eget quam adipiscing in vulputate ante ullamcorper. Sed eros ante, lacinia et sollicitudin et, aliquam sit amet augue. In hac habitasse platea dictumst.

2.1.2 Subsection 2

Morbi rutrum odio eget arcu adipiscing sodales. Aenean et purus a est pulvinar pellentesque. Cras in elit neque, quis varius elit. Phasellus fringilla, nibh eu tempus venenatis, dolor elit posuere quam, quis adipiscing urna leo nec orci. Sed nec nulla auctor odio aliquet consequat. Ut nec nulla in ante ullamcorper aliquam at sed dolor. Phasellus fermentum magna in augue gravida cursus. Cras sed pretium lorem. Pellentesque eget

ornare odio. Proin accumsan, massa viverra cursus pharetra, ipsum nisi lobortis velit, a malesuada dolor lorem eu neque.

2.2 Main Section 2

Sed ullamcorper quam eu nisl interdum at interdum enim egestas. Aliquam placerat justo sed lectus lobortis ut porta nisl porttitor. Vestibulum mi dolor, lacinia molestie gravida at, tempus vitae ligula. Donec eget quam sapien, in viverra eros. Donec pellentesque justo a massa fringilla non vestibulum metus vestibulum. Vestibulum in orci quis felis tempor lacinia. Vivamus ornare ultrices facilisis. Ut hendrerit volutpat vulputate. Morbi condimentum venenatis augue, id porta ipsum vulputate in. Curabitur luctus tempus justo. Vestibulum risus lectus, adipiscing nec condimentum quis, condimentum nec nisl. Aliquam dictum sagittis velit sed iaculis. Morbi tristique augue sit amet nulla pulvinar id facilisis ligula mollis. Nam elit libero, tincidunt ut aliquam at, molestie in quam. Aenean rhoncus vehicula hendrerit.

Chapter 3

Approach and direct formulation of noise analysis

3.1 Direct formulation of noise analysis

The intention behind this study is to perform a flow field noise analysis in CFD without implementation of acoustical analogies to the CFD code itself. Moreover, very limited information on direct formulation of noise analysis was found during the research, with even fewer research on acoustical near field of transonic axial compressors or axial fans of twin spool jet engines.

The process for the direct formulation noise analysis is following:

1. Obtain raw flow field data of static pressure, velocity magnitude from CFD analysis.
2. Perform averaging over time of pressure and velocity magnitude for each point or cell in the flow field (equation 3.1).
3. Obtain offset from mean static pressure and velocity magnitude for every timestep for every point/cell in the saved flow field (equation 3.2).

$$\bar{p} = \frac{1}{n}\sum_{i=1}^{n} p_i \qquad and \qquad \bar{u} = \frac{1}{n}\sum_{i=1}^{n} u_i \tag{3.1}$$

$$p_{i\ sound} = p_i - \bar{p} \qquad and \qquad u_{particle} = u_i - \bar{u} \tag{3.2}$$

Sound pressure signal and flow velocity offset is obtained for every node or cell centroid throughout the simulation flowtime. This dataset can be now post processed Dataset obtained in described manner now contains sound pressure of the flow field in

every mesh node or cell centroid throughout the computational time. The dataset is now post processed to obtain quantity information of the acoustic nearfield.

RMS sound pressure level can be obtained from the sound pressure data with use of the formula 3.3.

$$p_{rms} = \sqrt{\frac{\sum_{i=1}^{n} p_{i\ sound}^2}{n}} \tag{3.3}$$

Sound pressure decibel level (SPLdB) is compuded using formula 3.4 with standard reference pressure $p_{ref} = 0.00002Pa$.

$$SPLdB = 20 \cdot \log_{10}\left(\frac{|p_{i\ sound}|}{p_{ref}}\right) \tag{3.4}$$

3.2 CFD analysis requirements

References [2], [3], [1] and [4] provide a theoretical insight on generating sound in fluid flow due to shear mixing of flows or by implementing a solid boundary in the flow. General remark is: any source of turbulence that result in pressure fluctuation will result in generating sound. Therefore the main requirement for used CFD code for direct noise analysis is the capability of resolving turbulent flow and corresponding fluctuations of the pressure and density.

This approach requires using a finite volume method (fvm) CFD analysis.

3.3 Mesh sizing requirements

Let's assume a sinusoidal pressure fluctuation $y(t)$ (equation 3.5 of ordinary frequency of f and amplitude A moving through ambient medium, for more than 5 cycles at speed of sound 3.6. The mathematical and numerical methods for solving flow field described in section above are capable of computing such pressure fluctuation in a fine resolution mesh.

$$y(t) = Asin(2\pi ft + \phi) \tag{3.5}$$

$$a = \sqrt{\kappa RT} \tag{3.6}$$

Both cell size and time step size are limited by the wave length, and therefore frequency of the discussed pressure fluctuation. The wavelength is calculated by formula 3.7.

$$\lambda = \frac{v}{f} \tag{3.7}$$

Considered fluctuation travels through the finite volumes in the stationary CFD mesh. Pressure value is measured at the cell center for each timestep. At this stage, it is assumed that timestep is "good enough" for the analysis. Four possibilities are to be discussed

Scenario 1: wavelength is smaller than the edge length of the cell in the direction of propagation. In this condition, the pressure fluctuation performs a number of cycles within one cell (Fig. 3.1). Due to the numerical approach, such fluctuation will not be computed and recorded by data acquisition at the cell centroid or at node coordinates.

FIGURE 3.1: Scenario 1. Wavelength smaller than cell edge length

Scenario 2: wavelength and cell edge length in the direction of propagation are equal. In this condition, the pressure fluctuation performs one cycle within one cell in the direction of the fluctuation propagation (Fig. 3.2). Such pressure change will be also filtered out by the numerical scheme.

FIGURE 3.2: Scenario 2. Wavelength equal to cell edge length

Scenario 3: wavelength is equal to 4 minimum cell lengths in the direction of propagation. This is the minimum cell size condition for discussed approach. In this condition, the pressure fluctuation performs one cycle within four cells in the direction of the fluctuation propagation (Fig. 3.3). FVM method is now capable of computing the pressure resulting from sound wave propagation.

FIGURE 3.3: Scenario 3. Wavelength equal four minimum edge lengths

Scenario 4: wavelength is larger than 4 minimum cell edge lengths. In this condition, the pressure fluctuation performs one cycle within multiple cells in the direction of the fluctuation propagation (Fig. 3.4). FVM method computes pressure from the sound wave propagation across multiple cells.

FIGURE 3.4: Scenario 4. Wavelength larger than four minimum edge lengths

Based on these possibilities, the edge sizing of the finite volume cell should be at least four times smaller than the shortest wavelength expected in the flow field.

As there is no information on the pressure fluctuations in the flow field, the range of the further analyses will be limited to audible range of 20Hz to 20 000Hz. The wavelengths are calculated by formula 3.7 and divided by four to obtain the required cell sizing. The velocity of sound obtained by equation 3.6 with reference temperature $T = 300K$. The results for outermost sound frequencies of the audible range are presented in table 3.1

TABLE 3.1: Test case boundary conditions

Frequency [Hz]	Wave length [m]	Cell size [m]
20	17.390	4.347
20 000	0.01739	0.004347

3.4 Timestep requirements

There are two limiting factors for timestep requirements. The high frequency signal is limited by the timestep size, whereas the low frequencies are limited to the total number of timesteps and physical flow time calculated. The timestep size is calculated first.

Once sizing of the mesh is established, time at which the fluctuation passes the cell is established by simple formula 3.8. Distance s is the cell edge sizing, obtained as in section 3.3 and the relation between cell size and wave length is presented in equation 3.10.

$$a = \frac{s}{t} \tag{3.8}$$

Where

$$t = \frac{1}{f} \tag{3.9}$$

$$s = \frac{\lambda}{4} \tag{3.10}$$

By rearranging the equation 3.8 to solve for t and substituting λ by 3.7 we obtain:

$$t = \frac{s}{a} = \frac{\lambda}{4a} = \frac{a}{f} \cdot \frac{1}{4a} = \frac{1}{4f} \tag{3.11}$$

Equation 3.11 shows that time step for the analysis is dependent from the expected value of high frequency fluctuations. Four scenarios can be discussed.

Scenario 1: timestep is smaller than 1/4 of the fluctuation period (Fig. 3.5).

Scenario 2: timestep is equal to the 1/4 of the fluctuation period (Fig. 3.6).

Scenario 3: timestep is equal to fluctuation period (Fig. 3.7).

Scenario 4: timestep is larger that fluctuation period (Fig. 3.8).

In order to capture frequencies on the low end of the spectrum, the analysis must be performed long enough to capture at least a single, with optimum 5 or more periods, of the desired low frequency. Assuming lower end of the audible frequency spectrum,

FIGURE 3.5: Scenario 1. Timestep smaller than 1/4 of fluctuation period

FIGURE 3.6: Scenario 2. Timestep equal to 1/4 of fluctuation period

FIGURE 3.7: Scenario 3. Timestep equal to fluctuation period

the 20Hz frequency, the simulation time must resemble at least 0.05s of flow time with optimum 0.25s of flow time at given timestep.

3.5 Limiting factors of the direct approach

Provided approach is solely a post processing approach relying on data provided by a CFD analysis. In order to obtain reasonable results down the process, the analysis itself

FIGURE 3.8: Scenario 4. Timestep is larger than fluctuation period

mus be capable of delivering pressure fluctuations that can be considered as acoustic in source.

Utilizing a numerical model that averages flow field in terms of numerical methods, treatment of turbulent motions or mesh of insufficient quality, will return a pressure flow field that all acoustic kind fluctuations filtered out.

Pressure signal used by this approach is given by a list of real scalar values for each node or cell centroid for each timestep. Therefore obtaining phase shift of the ordinary sinuses components of pressure signal may be challenging, if at all possible, and relies solely on further postprocessing of generated data.

The range of frequencies captured by this method depends on the mesh sizing and timestep sizing. Therefore, if the range of expected frequencies is known or at least estimated, the mesh sizing and timestep size can be adjusted for the given case.

Direct formulation acoustic analysis requires storing pressure and velocity information from all timesteps and then performing averaging over all timesteps. For analysis within audible range 4000 timesteps is required for one 20Hz period. Considering the mesh sizing requirements, the mesh cell count will rise up to tens of millions, which makes storing and managing the data somewhat difficult. Averaging the timestep data, obtaining sound pressure levels, sound intensity levels and respective decibel levels.

For incompressible flows or flows with low pressure gradients or without shock waves such approach is exaggerated. Should the flow occur in majority in ambient conditions (i.e. low velocity jet in free stream), the offset from the ambient pressure may be computed "on-the-fly".

Although computationally expensive, such approach is required in flows with very high pressure gradients, as it is impossible to establish one reference pressure for whole flow field.

Chapter 4

Test case

4.1 NASA Rotor 67 transonic axial compressor

The test specimen for given analysis is a NASA Rotor 67 (R67) transonic axial compressor. Originating as a first stage of two stage fan for evaluation of design procedures, validation of experimental facilities as well as meshing and CFD tools. Both stages were used in a multitude of studies for aerodynamics, geometry optimisation, noise analyses and structural analyses. Full design procedure can be found in references [5] and [6]. The CFD analysis and further post processing of the pressure signals shall be performed on a single passage of a first stage rotor of the compressor. The setup for the calculations (apart from the single passage constraint) is relevant do case described in [7], which was the main source for geometry and flowfield data.

Basic figures of the given rotor are, design pressure ratio of 1.63 at massflow of 33.25 kg/sec. The design rotational speed is 16 043 rpm, which yields a tip speed of 429 m/s and an inlet tip relative Mach number of 1.38. The rotor has 22 blades and an aspect ratio of 1.56 (based on average span/root axial chord). The inlet and exit tip diameters are 514 and 485 mm, respectively, and the inlet and exit hub/tip radius ratios are 0.375 and 0.478, respectively. A fillet radius of 1.78 mm is used at the airfoil-hub juncture. The square root of the mean square of the airfoil surface finish is 0.8 μm or better, the airfoil surface tolerance is $\pm$ 0.04 mm, and the running tip clearance is approximately 1.0 mm [7]. Surface roughness and some of the geometrical features are omitted during the preparation of the geometry and CFD mesh for reasons described in sections 4.2 and 4.3. General geometry of NASA R67 is presented on fig 4.1

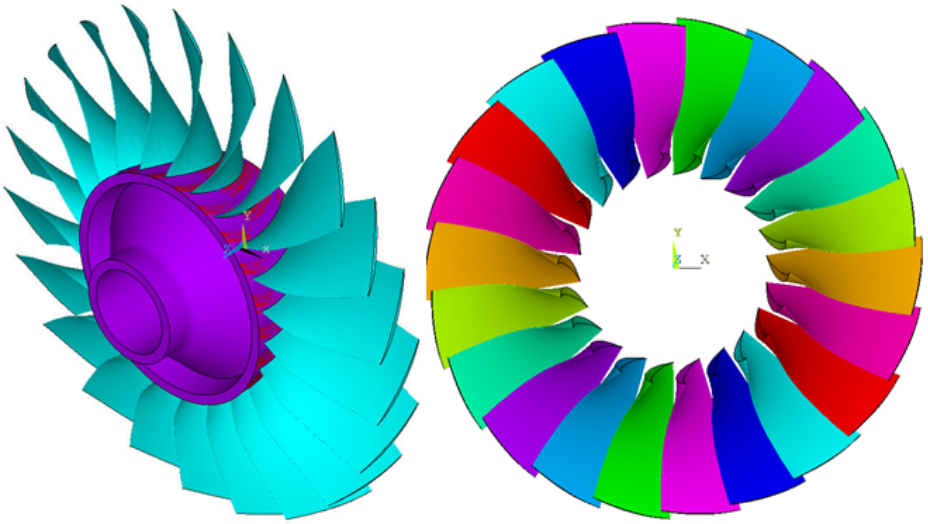

FIGURE 4.1: Geometry of NASA R67

4.2 3D geometry preparation

Geometry was prepared in Ansys ICEM 14.5 meshing software. Creating the geometry directly in the meshing software reduces the risk of creating flaws in the geometry, due to file translations. Mesh is created in millimeters.

The R67 blade coordinates for rotor and stator on both stages is given in references [5] and [6] and provide the blade elements in a Multiple-Circular-Arc fashion. In such approach the design blade elements lie on conical surfaces which approximate the actual stream flow surfaces. A blade-element-layout method is developed which preserves the constant-angle change characteristic of the circular-arc profile. More specifically, the mean camber line and the suction and pressure surface lines of a blade element are lines with a constant rate of angle change with path distance on a specified conical surface [8]. Although relatively comfortable for design purposes, such approach requires implementing a macro or script to desired CAD tool for creating the blade elements or transforming the MCA blade to Cartesian or cylindrical coordinates. Reference [8] provides an extended definition of MCA blade description as well as Fortran code for generating blade cross-section and geometric properties of the blade. Source [7] provides a list of coordinates for 14 profiles of the 1st stage rotor blade suction and pressure side, as well as coordinates for hub and casing int the meridional plane. These coordinates were used to create the geometry of the single passage of the subject blade. Coordinates are also available in Appendix C and project Github repository [9].

The coordinate system is a standard right-hand Cartesian CS. Rotation axis is set to Z-axis with flow in positive Z direction. The compressor rotation is set as in right-hand rule, the compressor rotates in clockwise direction when facing the blade leading edge.

$Z = 0$ coordinate is defined by point number 1 on 1st blade design surface (see Appendix C for details).

Hub and casing flow path were created by importing formatted point data as a b-spline curve, followed by extrusion the curve to surface by rotating it by ±60°. Blade surfaces cylindrical coordinates were transformed to Cartesian coordinates using simple trigonometric calculations and imported as set of splines. Suction and pressure surface of the blade were created by lofting the surface along the imported splines. Leading and trailing edge radii were created in a similar manner with use of edge radius and edge tangency points given in [7]. Tip gap of the blade was created by offsetting the casing surface by 1.016 mm in the normal direction towards the rotation axis and creating a section line between blade surfaces and the offset surface.

Due to the estimated mesh cell count, only one blade passage is created, therefore a set of periodic surfaces must be defined. ICEM software is capable of creating a midline as an average of coordinates of two given lines. A midline was created for every design profile and was manually extended beyond the blade leading and trailing edge. Midlines were lofted to create a midsurface which was later on copied with rotation by $\pm 0.5 \cdot \frac{360°}{22}$ to create two identical periodic surfaces.

Aforementioned midlines were also rotated along Z-axis to create control surfaces for mesh stabilization and data acquisition down the process.

Reference [7] provides coordinates of hub and casing for the full experiment, however only a rotating part of the experimental rotor setup will be used. Two surfaces normal to Z direction at coordinates Z = -13.74 mm and Z = 93.65 mm are placed as inlet and outlet boundary conditions. Geometry was finished by necessary extrusions, trimming and other finishing operations to ensure high quality surface for meshing. Usually, the geometry must be watertight to ensure proper meshing process, however ICEM as patch-independent meshing software does not require that.

Physical experiment test compressor has a 1.78 mm fillet at airfoil-hub juncture. This feature was omitted as it would unnecessarily complicate the meshing process and increase the cell count.

Such approach allowed for creating a geometry for single blade passage with centered blade of 1st stage rotor of the test compressor (Fig 4.2).

4.3 Meshing approach

Following requisites are posed to the mesh for the discussed case:

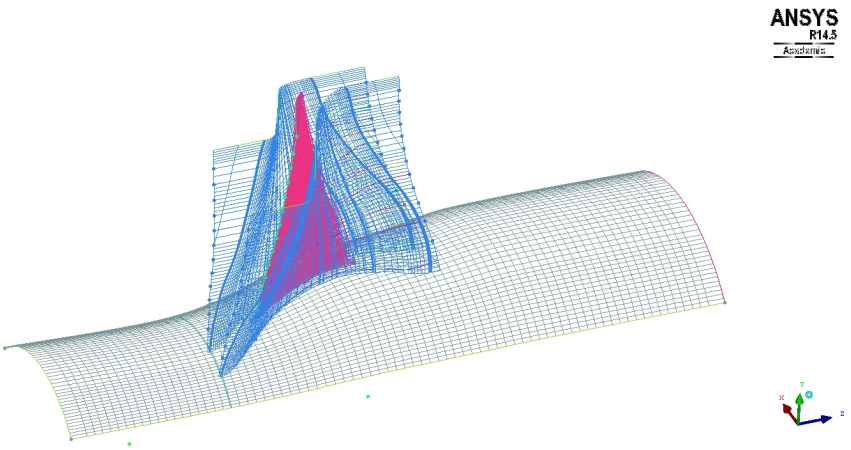

FIGURE 4.2: Final single passage geometry. Some features hidden for clarity

- Possibly low number of elements fulfilling the mesh sizing requirements stated in chapter 3.1,
- Mesh should be a fully structural mesh including the tip gap,
- The periodic boundary mesh must be identical/conforming for both boundaries,
- The mesh must have high quality metrics in terms of cell orthogonality and skew as defined by equations 4.1 & 4.2 respectively.

$$Orthogonality = \frac{\vec{A}_i \cdot \vec{f}_i}{|\vec{A}_i| \cdot |\vec{f}_i|} \tag{4.1}$$

$$Skewness = \frac{OptimalCellSize - CellSize}{OptimalCellSize} \tag{4.2}$$

One of the initial mesh concepts was an unstructured mesh with triangular surface mesh extruded to prism boundary layer and mostly isotropic tetrahedra in the volume. This approach was quickly rejected for bad quality elements near the airfoil/hub junction and tip gap, as well as element count in range of 4.5 million cells for sizing relevant for RANS analysis. This approach was quickly dropped.

A non-trivial topology with fully conforming periodic boundaries was introduced (fig 4.3). This topology fulfills all the prerequisites stated apart from possibility to mesh a structural tip gap. Such approach makes it impossible from topological standpoint to place a structural mesh in this area. A RANS sufficient mesh without tip gap area (blade was extended to the casing surface) was created. The cell count for this mesh is below 0.5 million cells with better skewness and orthogonal quality. This mesh was utilized for numerical setup and data acquisition testing as it was faster to converge.

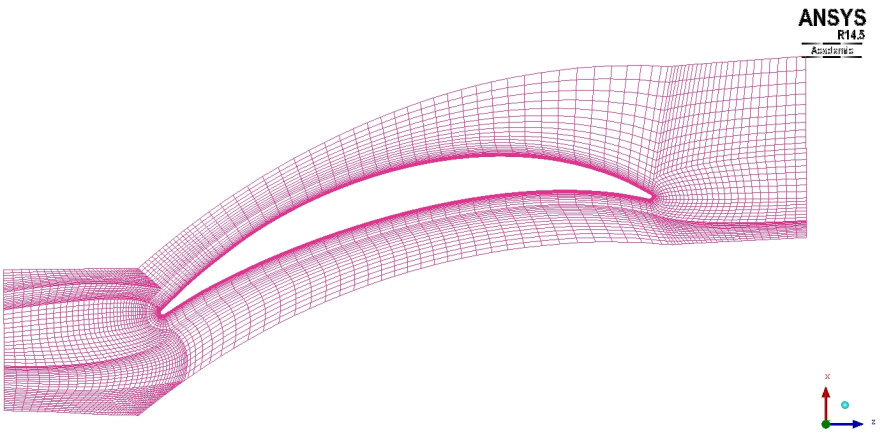

FIGURE 4.3: Mesh topology with conforming periodic boundaries

Final topology was a standard h-grid topology for airfoil 4.4. Although it is impossible to create a conforming periodic interface with such mesh topology, a fully structural tip gap was implemented. Omitting the blade-hub juncture fillet simplified the mesh. Such topology eradicates the necessity of placing 5-way topology points.

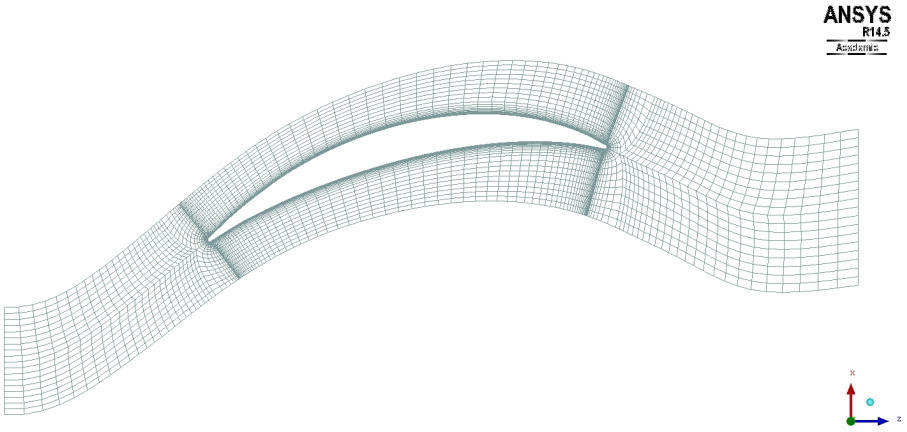

FIGURE 4.4: Mesh h-topology

Mesh was created in Ansys ICEM software using structural blocking method. The topology was sliced and associated to internal surfaces mentioned in the above section. This enforces mesh layering along design streamlines and provides high quality mesh on internal surfaces for flow field data acquisition further in the process. Blade wall boundary condition is distributed among five separate parts: blade pressure side, blade suction side, leading and trailing edges and tip surface.

Element sizing in volume and in tangent direction to the blade is limited to 3 mm, with 5 mm at inlet and outlet boundary conditions. The mesh sizing requirements are described in chapter 3. Blade boundary layer is produced by creating an o-grid around blade geometry. Hub and casing boundary layers are created by changing the sizing on

the blocks adjacent to the geometry. Sizing of the first element is estimated with y+ parameter as described in equation: 4.3. First element thickness in on the blade surfaces ranges from is $2\mu m$ on tip airfoil and $10\mu m$ on hub airfoil. This corresponds to $y^+ \approx 2$ calculated by streamline velocity values given in [7].

$$\Delta s = \frac{y^+ \mu}{U_{fric} \rho} \tag{4.3}$$

Where:

$$U_{fric} = \sqrt{\frac{\tau_{wall}}{\rho}} \tag{4.4}$$

Where:

$$\tau_{wall} = \frac{C_f \rho U_{\inf}^2}{2} \tag{4.5}$$

Where:

$$C_f = \frac{0.026}{Re_x^{1/7}} \tag{4.6}$$

Figure 4.5, provides overview of mesh quality defined by figure 4.1. Created mesh is of high quality and is sufficient for both RANS (chapter 5) and DDES (chapter 6) analyses. Final mesh reached roughly 11.5 million cell count. Final mesh is presented in figure 4.6

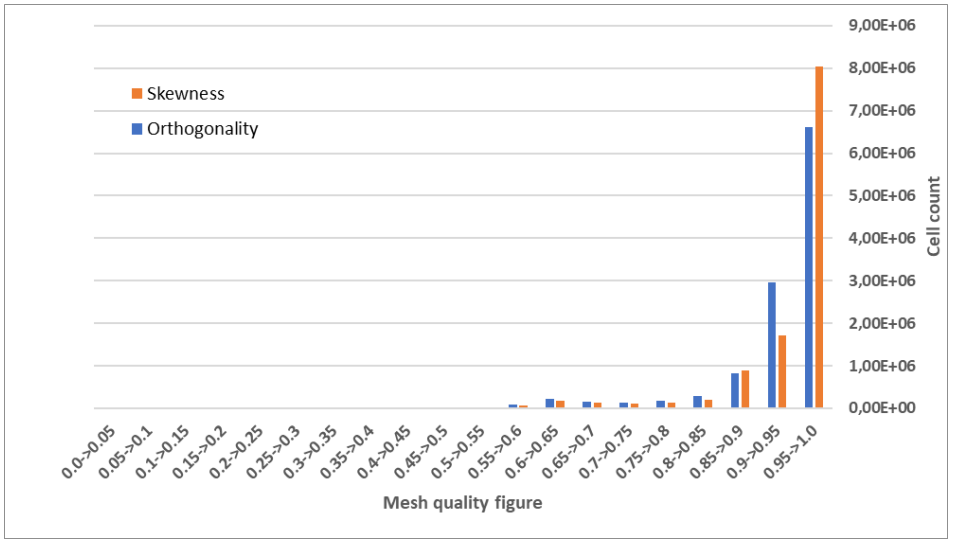

FIGURE 4.5: Mesh non-orthogonality histogram

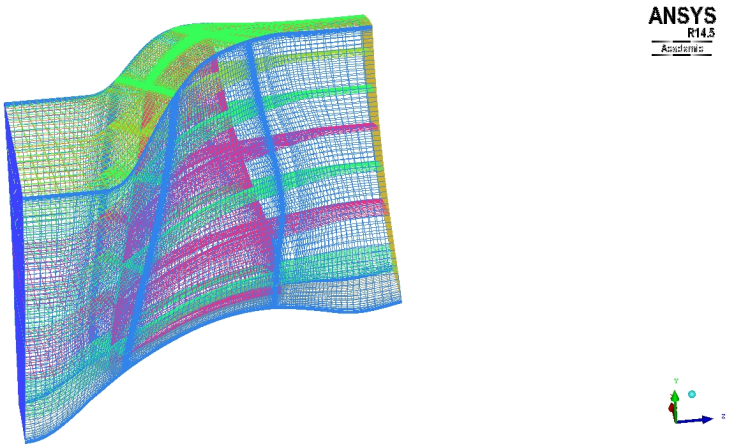

FIGURE 4.6: Completed Mesh

4.4 Case preprocessing

CFD analyses for generating raw pressure field data are performed in ANSYS Fluent 17.2 software on Prometheus HPC cluster located in Kraków. Access for this infrastructure was granted by PLGrid infrastructure. Calculations were run on 5 nodes of 24CPU cores and 128GB RAM each [10], which resulted in decomposition to 120 cores, resulting in allocating around 110 thousand cells to a single HPC core.

Following is the numerical setup for all of the performed analyses. The setup corresponds to "peak efficiency conditions" of the experimental compressor.

4.4.1 General settings and material properties

Analysis was resolved using implicit density based solver. The theory behind the solver is described in chapter 3. Material used in the anaysis resembles standard air modeled as ideal gas as in equation with following properties described in table 4.1

TABLE 4.1: Standard air properties

C_p	1006.43	$\frac{J}{kg \cdot K}$
λ	0.0242	$\frac{W}{m \cdot K}$
μ	1.7894e-05	$\frac{kg}{m \cdot s}$
M	28.966	$\frac{kg}{kmol}$

$$pV = nRT \tag{4.7}$$

Analysis operating pressure is set to 0 Pascal, which is a standard practice in compressible flow CFD.

Fluid zone is set as "frozen rotor" - rotating reference frame. Although no mesh motion is implied, the effect of Coriolis accelerations and centrifugal acceleration will be taken into account by adding respective acceleration components to momentum equations as described in chapter 3. The rotational velocity is set to 1680 rad/s.

4.4.2 Boundary conditions

Following boundary conditions were applied to the mesh boundaries. Following setup is again typical for compressible flow CFD.

TABLE 4.2: Test case boundary conditions

Boundary marker	Boundary type		
Inlet	Pressure Inlet	101350	Pa
Outlet	Pressure Outlet	102000	Pa
Hub	Movig wall	1680	rad/s
Blade	Moving wall	1680	rad/s
Casing	Stationary wall		
Internal profiles	Internal		
Periodic boundaries	Interface		

Moving wall boundaries represent the rotational velocity of the compressor blade and are necessary for stationary reference frame formulation. Boundary condition setup is no different to usual setups of analyses of such kind.

4.5 Data acquisition

Mesh and case is set up for possibly efficient data acquisition of flow field pressure and velocity data. FLUENT data file from a single timestep takes around 2GB of disk space. Saving such dataset from every of 50150 timesteps requires about 97TB of storage, which was unavailable at the time.

Data was gathered from blade surface (5 boundary markers) and 13 internal markers. Following node data values were saved:

- Static pressure
- Velocity magnitude (only internal markers)
- Vorticity magnitude (only internal markers)
- Static density
- Static temperature

- Node coordinates

This approach generated 18 datasets of 50510 files each, resulting in taking up 5.5TB of HPC cluster storage. The number of data is still large but manageable with current software engineering tools. Data was saved to ASCII text files.

Chapter 5

RANS Analysis

5.1 Main Section 1

Lorem ipsum dolor sit amet, consectetur adipiscing elit. Aliquam ultricies lacinia euismod. Nam tempus risus in dolor rhoncus in interdum enim tincidunt. Donec vel nunc neque. In condimentum ullamcorper quam non consequat. Fusce sagittis tempor feugiat. Fusce magna erat, molestie eu convallis ut, tempus sed arcu. Quisque molestie, ante a tincidunt ullamcorper, sapien enim dignissim lacus, in semper nibh erat lobortis purus. Integer dapibus ligula ac risus convallis pellentesque.

5.1.1 Subsection 1

Nunc posuere quam at lectus tristique eu ultrices augue venenatis. Vestibulum ante ipsum primis in faucibus orci luctus et ultrices posuere cubilia Curae; Aliquam erat volutpat. Vivamus sodales tortor eget quam adipiscing in vulputate ante ullamcorper. Sed eros ante, lacinia et sollicitudin et, aliquam sit amet augue. In hac habitasse platea dictumst.

5.1.2 Subsection 2

Morbi rutrum odio eget arcu adipiscing sodales. Aenean et purus a est pulvinar pellentesque. Cras in elit neque, quis varius elit. Phasellus fringilla, nibh eu tempus venenatis, dolor elit posuere quam, quis adipiscing urna leo nec orci. Sed nec nulla auctor odio aliquet consequat. Ut nec nulla in ante ullamcorper aliquam at sed dolor. Phasellus fermentum magna in augue gravida cursus. Cras sed pretium lorem. Pellentesque eget ornare odio. Proin accumsan, massa viverra cursus pharetra, ipsum nisi lobortis velit, a malesuada dolor lorem eu neque.

5.2 Main Section 2

Sed ullamcorper quam eu nisl interdum at interdum enim egestas. Aliquam placerat justo sed lectus lobortis ut porta nisl porttitor. Vestibulum mi dolor, lacinia molestie gravida at, tempus vitae ligula. Donec eget quam sapien, in viverra eros. Donec pellentesque justo a massa fringilla non vestibulum metus vestibulum. Vestibulum in orci quis felis tempor lacinia. Vivamus ornare ultrices facilisis. Ut hendrerit volutpat vulputate. Morbi condimentum venenatis augue, id porta ipsum vulputate in. Curabitur luctus tempus justo. Vestibulum risus lectus, adipiscing nec condimentum quis, condimentum nec nisl. Aliquam dictum sagittis velit sed iaculis. Morbi tristique augue sit amet nulla pulvinar id facilisis ligula mollis. Nam elit libero, tincidunt ut aliquam at, molestie in quam. Aenean rhoncus vehicula hendrerit.

Chapter 6

DDES Analysis

6.1 Main Section 1

Lorem ipsum dolor sit amet, consectetur adipiscing elit. Aliquam ultricies lacinia euismod. Nam tempus risus in dolor rhoncus in interdum enim tincidunt. Donec vel nunc neque. In condimentum ullamcorper quam non consequat. Fusce sagittis tempor feugiat. Fusce magna erat, molestie eu convallis ut, tempus sed arcu. Quisque molestie, ante a tincidunt ullamcorper, sapien enim dignissim lacus, in semper nibh erat lobortis purus. Integer dapibus ligula ac risus convallis pellentesque.

6.1.1 Subsection 1

Nunc posuere quam at lectus tristique eu ultrices augue venenatis. Vestibulum ante ipsum primis in faucibus orci luctus et ultrices posuere cubilia Curae; Aliquam erat volutpat. Vivamus sodales tortor eget quam adipiscing in vulputate ante ullamcorper. Sed eros ante, lacinia et sollicitudin et, aliquam sit amet augue. In hac habitasse platea dictumst.

6.1.2 Subsection 2

Morbi rutrum odio eget arcu adipiscing sodales. Aenean et purus a est pulvinar pellentesque. Cras in elit neque, quis varius elit. Phasellus fringilla, nibh eu tempus venenatis, dolor elit posuere quam, quis adipiscing urna leo nec orci. Sed nec nulla auctor odio aliquet consequat. Ut nec nulla in ante ullamcorper aliquam at sed dolor. Phasellus fermentum magna in augue gravida cursus. Cras sed pretium lorem. Pellentesque eget ornare odio. Proin accumsan, massa viverra cursus pharetra, ipsum nisi lobortis velit, a malesuada dolor lorem eu neque.

6.2 Main Section 2

Sed ullamcorper quam eu nisl interdum at interdum enim egestas. Aliquam placerat justo sed lectus lobortis ut porta nisl porttitor. Vestibulum mi dolor, lacinia molestie gravida at, tempus vitae ligula. Donec eget quam sapien, in viverra eros. Donec pellentesque justo a massa fringilla non vestibulum metus vestibulum. Vestibulum in orci quis felis tempor lacinia. Vivamus ornare ultrices facilisis. Ut hendrerit volutpat vulputate. Morbi condimentum venenatis augue, id porta ipsum vulputate in. Curabitur luctus tempus justo. Vestibulum risus lectus, adipiscing nec condimentum quis, condimentum nec nisl. Aliquam dictum sagittis velit sed iaculis. Morbi tristique augue sit amet nulla pulvinar id facilisis ligula mollis. Nam elit libero, tincidunt ut aliquam at, molestie in quam. Aenean rhoncus vehicula hendrerit.

Chapter 7

Results of flow field noise analysis

7.1 Main Section 1

Lorem ipsum dolor sit amet, consectetur adipiscing elit. Aliquam ultricies lacinia euismod. Nam tempus risus in dolor rhoncus in interdum enim tincidunt. Donec vel nunc neque. In condimentum ullamcorper quam non consequat. Fusce sagittis tempor feugiat. Fusce magna erat, molestie eu convallis ut, tempus sed arcu. Quisque molestie, ante a tincidunt ullamcorper, sapien enim dignissim lacus, in semper nibh erat lobortis purus. Integer dapibus ligula ac risus convallis pellentesque.

7.1.1 Subsection 1

Nunc posuere quam at lectus tristique eu ultrices augue venenatis. Vestibulum ante ipsum primis in faucibus orci luctus et ultrices posuere cubilia Curae; Aliquam erat volutpat. Vivamus sodales tortor eget quam adipiscing in vulputate ante ullamcorper. Sed eros ante, lacinia et sollicitudin et, aliquam sit amet augue. In hac habitasse platea dictumst.

7.1.2 Subsection 2

Morbi rutrum odio eget arcu adipiscing sodales. Aenean et purus a est pulvinar pellentesque. Cras in elit neque, quis varius elit. Phasellus fringilla, nibh eu tempus venenatis, dolor elit posuere quam, quis adipiscing urna leo nec orci. Sed nec nulla auctor odio aliquet consequat. Ut nec nulla in ante ullamcorper aliquam at sed dolor. Phasellus fermentum magna in augue gravida cursus. Cras sed pretium lorem. Pellentesque eget ornare odio. Proin accumsan, massa viverra cursus pharetra, ipsum nisi lobortis velit, a malesuada dolor lorem eu neque.

7.2 Main Section 2

Sed ullamcorper quam eu nisl interdum at interdum enim egestas. Aliquam placerat justo sed lectus lobortis ut porta nisl porttitor. Vestibulum mi dolor, lacinia molestie gravida at, tempus vitae ligula. Donec eget quam sapien, in viverra eros. Donec pellentesque justo a massa fringilla non vestibulum metus vestibulum. Vestibulum in orci quis felis tempor lacinia. Vivamus ornare ultrices facilisis. Ut hendrerit volutpat vulputate. Morbi condimentum venenatis augue, id porta ipsum vulputate in. Curabitur luctus tempus justo. Vestibulum risus lectus, adipiscing nec condimentum quis, condimentum nec nisl. Aliquam dictum sagittis velit sed iaculis. Morbi tristique augue sit amet nulla pulvinar id facilisis ligula mollis. Nam elit libero, tincidunt ut aliquam at, molestie in quam. Aenean rhoncus vehicula hendrerit.

Chapter 8

Conclusions & Further work

8.1 Main Section 1

Lorem ipsum dolor sit amet, consectetur adipiscing elit. Aliquam ultricies lacinia euismod. Nam tempus risus in dolor rhoncus in interdum enim tincidunt. Donec vel nunc neque. In condimentum ullamcorper quam non consequat. Fusce sagittis tempor feugiat. Fusce magna erat, molestie eu convallis ut, tempus sed arcu. Quisque molestie, ante a tincidunt ullamcorper, sapien enim dignissim lacus, in semper nibh erat lobortis purus. Integer dapibus ligula ac risus convallis pellentesque.

8.1.1 Subsection 1

Nunc posuere quam at lectus tristique eu ultrices augue venenatis. Vestibulum ante ipsum primis in faucibus orci luctus et ultrices posuere cubilia Curae; Aliquam erat volutpat. Vivamus sodales tortor eget quam adipiscing in vulputate ante ullamcorper. Sed eros ante, lacinia et sollicitudin et, aliquam sit amet augue. In hac habitasse platea dictumst.

8.1.2 Subsection 2

Morbi rutrum odio eget arcu adipiscing sodales. Aenean et purus a est pulvinar pellentesque. Cras in elit neque, quis varius elit. Phasellus fringilla, nibh eu tempus venenatis, dolor elit posuere quam, quis adipiscing urna leo nec orci. Sed nec nulla auctor odio aliquet consequat. Ut nec nulla in ante ullamcorper aliquam at sed dolor. Phasellus fermentum magna in augue gravida cursus. Cras sed pretium lorem. Pellentesque eget ornare odio. Proin accumsan, massa viverra cursus pharetra, ipsum nisi lobortis velit, a malesuada dolor lorem eu neque.

8.2 Main Section 2

Sed ullamcorper quam eu nisl interdum at interdum enim egestas. Aliquam placerat justo sed lectus lobortis ut porta nisl porttitor. Vestibulum mi dolor, lacinia molestie gravida at, tempus vitae ligula. Donec eget quam sapien, in viverra eros. Donec pellentesque justo a massa fringilla non vestibulum metus vestibulum. Vestibulum in orci quis felis tempor lacinia. Vivamus ornare ultrices facilisis. Ut hendrerit volutpat vulputate. Morbi condimentum venenatis augue, id porta ipsum vulputate in. Curabitur luctus tempus justo. Vestibulum risus lectus, adipiscing nec condimentum quis, condimentum nec nisl. Aliquam dictum sagittis velit sed iaculis. Morbi tristique augue sit amet nulla pulvinar id facilisis ligula mollis. Nam elit libero, tincidunt ut aliquam at, molestie in quam. Aenean rhoncus vehicula hendrerit.

Appendix A

Code for direct formulation of noise analysis

Write your Appendix content here.

Appendix B

Code for discrete Fourier analysis

Write your Appendix content here. [2] [3] [4] [1] [8] [5] [6] [7]

Appendix C

Blade design surface coordinates

Write your Appendix content here. [2] [3] [4] [1] [8] [5] [6] [7]

Bibliography

[1] D. L. Hawkings J. E. Ffowcs Williams. Sound generation by turbulence and surfaces in arbitrary motion. *Philosophical Transactions of the Royal Society of London. Series A, Mathematical and Physical Sciences*, 264(1151):321–342, May 1969. URL http://www.jstor.org/stable/73790.

[2] M. J. Lighthill. On sound generated aerodynamically i. general theory. *Proceedings of the Royal Society. Series A, Mathematical, Physical and Engineering Sciences*, 211 (1107):564–587, March 1952. URL http://rspa.royalsocietypublishing.org/content/211/1107/564.

[3] M. J. Lighthill. On sound generated aerodynamically ii. turbulence as a source of sound. *Proceedings of the Royal Society. Series A, Mathematical, Physical and Engineering Sciences*, 222(1148):1–32, March 1954. URL http://rspa.royalsocietypublishing.org/content/222/1148/1.

[4] N. Curle. The influence of solid boundaries upon aerodynamic sound. *Proceedings of the Royal Society. Series A, Mathematical, Physical and Engineering Sciences*, 231(1187):505–514, September 1955. URL http://rspa.royalsocietypublishing.org/content/231/1187/505.

[5] W. Stevans W. S. Cunnan and D. C. Urasek. Design and performance of a 427-meter-per-second-tip-speed two stage fan having a 2.40 pressure ratio. *NASA Technical Paper*, (TP-1314), October 1978.

[6] W. T. Gorrel D. C. Urasek and W. S. Cunnan. Performance of a two-stage fan having a low-aspect-ratio, first-stage rotor blading. *NASA Technical Paper*, (TP-1493), August 1979.

[7] M. D. Hathaway A. J. Strazisar, J. R. Wood and Kenneth L. Suder. Laser anemometer measurements in a transonic axial-flow fan rotor. *NASA Technical Paper*, (TP-2897), November 1989.

[8] J. S. David C. Janetzke J. E. Crouse and R. E. Schwirian. A computer program for composing blading from simulated circular-arc elements on conical surfaces. *NASA Technical Note*, (TN D-5437), September 1969.

[9] J. Mosiezny. Github repository for nasa r67 input data and noise analysis. 2018. URL `https://github.com/JedrzejMosiezny/R67-data-analysis`.

[10] Prometheus computation resources. 2018. URL `https://kdm.cyfronet.pl/portal/Prometheus`.